Inorganic Chemistry
Cite This: Inorg. Chem. 2018, 57, 2766−2772
Article
pubs.acs.org/IC

Temperature Effect on Co-Based Catalysts in Oxygen Evolution Reaction

Guangxing Zhang,[†] Han Wang,[†] Jinlong Yang, Qinghe Zhao, Luyi Yang, Hanting Tang, Chaokun Liu, Haibiao Chen, Yuan Lin, and Feng Pan*

School of Advanced Materials, Shenzhen Graduate School, Peking University, Shenzhen, 518055, P. R. China

Supporting Information

ABSTRACT: Oxygen evolution reaction (OER), as the critical step in splitting water, is a thermodynamically "up-hill" process and requires highly efficient catalysts to run. Arrhenius' law suggests that the higher temperature, the faster the reaction rate, so that a larger OER current density can be achieved at a lower η. Herein, we report an abnormal temperature effect on the performance of Co-based catalysts, e.g., Co_3O_4, Li_2CoSiO_4, and Fe-doped $Co(OH)_x$, in OER in alkaline electrolytes. The OER performance reached a maximum when the temperature increased to 65 °C, and the OER performance declined when the temperature became higher. The mechanism was investigated by using Co_3O_4 as a model sample, and we propose that at an optimal temperature (around 55−65 °C) the main rate-determining step changes from OH^- adsorption dominant to a mixed mode and both the adsorption and the cleavage of the OH group can be rate-determining, which leads to the fastest kinetics.

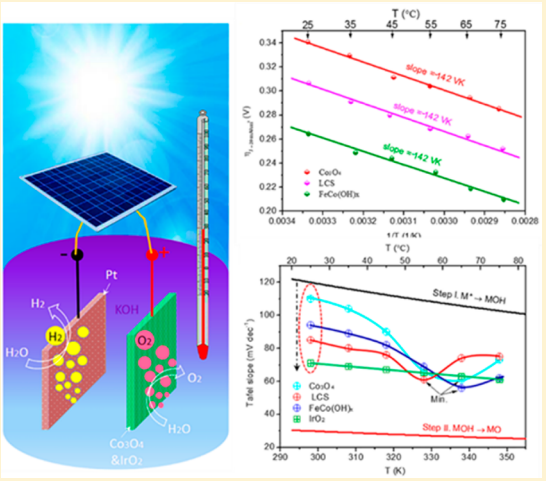

Oxygen evolution reaction (OER), as the critical step in splitting water into hydrogen and oxygen, is an environmentally friendly and effective approach for the production, storage, and usage of green energy including sustainable hydrogen production, rechargeable metal-air batteries, and fuel cells.[1−3] As a thermodynamically "up-hill" reaction, OER requires the input of energy to drive its completion.[4−6] In order to lower the reaction energy barrier, huge research efforts have focused on the discovery of increasingly efficient catalysts to accelerate the OER reaction kinetics (indicated by lowering the Tafel slope) at a low overpotential (η). The state-of-the-art OER catalysts include IrO_2[7] and RuO_2,[8] but the scarcity and high cost of these oxides of precious metals limit their large-scale application. Recently, transition metal (Fe, Co, Ni, Mn, etc.) compounds (including hydroxides,[28−30] oxides,[31,32] sulfides, phosphides, etc.) have attracted tremendous research interests, due to their Earth-abundant resource and comparable OER performance to that of precious metal oxides.[9−11]

So far, many research efforts have been made to improve the OER performance by the design and optimization of the catalyst structure. For example, multimetal doping transition metal oxides/hydroxides[12,13] can improve their conductivity and lower the energy barrier for OER. In addition, morphological control and design of a nano- and porous structure with a large surface area can create more OER active sites on the surface of the catalysts.[14,15] Apart from the catalyst itself, the support and the electrolyte are also important factors influencing the OER activity. For example, hybrid Co_3O_4/carbon nanowires directly grown on Cu foil yielded higher activity than unsupported catalyst.[15] In addition, Suntivich et al. observed that the OER activity depends on pH since the adsorption of OH and O (OH_{ad} and O_{ad}, respectively) is affected by pH.[16] A higher electrolyte pH appears to provide an additional activity boost.[17] Therefore, various strategies have been implemented to optimize the alkaline water splitting system which is a promising candidate for commercial hydrogen production as a strong alkaline condition relatively favors OER at a low cost.

In fact, the temperature of a water electrolysis device was known to reach as high as 65 °C naturally when utilizing the infrared range of the solar spectrum via photovoltaic cells,[18,19] while there were few reports on the effect of temperature on OER and related mechanisms on catalysts. A common understanding based on Arrhenius' law ($k = A\exp(-E_a/RT)$) is that the chemical reaction rate (k) depends on temperature (T) and the activation energy (E_a). The Arrhenius' law suggests that the higher the temperature, the faster the reaction rate so that one can obtain a larger OER current density at a lower η by raising the temperature. What will happen to how the catalyst promotes the OER process at different temperatures? Are there different mechanisms for different catalysts in a specific temperature range? Therefore, it is necessary to conduct a

Received: December 19, 2017
Published: February 22, 2018

DOI: 10.1021/acs.inorgchem.7b03168
Inorg. Chem. 2018, 57, 2766−2772

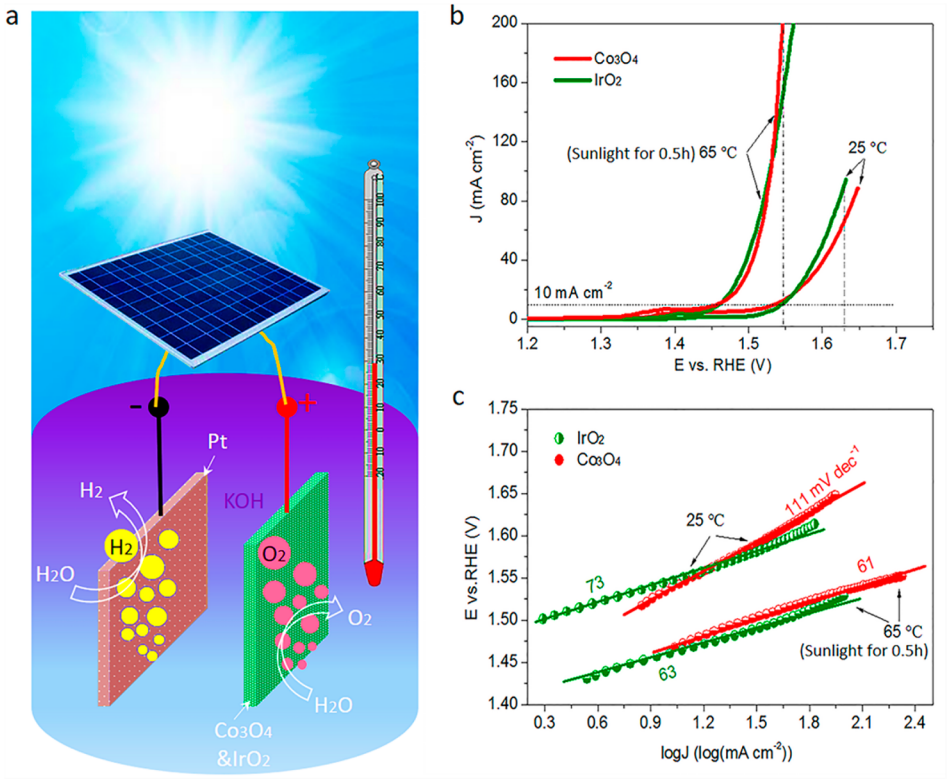

Figure 1. (a) Schematic diagram of an efficient, clean, and sustainable alkaline water electrolyzer, (b) compared linear scan voltammogram (LSV) curves at 2 mV s^{-1} and (c) Tafel plots of IrO_2 and Co_3O_4 catalysts in 1 M KOH at 25 and 65 °C.

systematical study on the effect of temperature, which will help to understand the nature of the catalytic behavior in OER and to guide practical application.

Herein, we present a study on the effect of the temperature on the OER performance of a commercial IrO_2 and a non-noble Co_3O_4 catalyst by exploiting their trends of η and the Tafel slopes with regard to the temperature. Specifically, IrO_2 catalyst showed a linear relationship between η and $1/T$ at all current densities, suggesting that the OER performance increased monotonically with the temperature. However, the Co_3O_4 catalyst behaved differently by showing maximum OER performance at a moderate temperature of 65 °C and declined performance when the temperature was higher. The trends of the Tafel slope showed that the different temperature effects on both catalysts can be attributed to their different rate-determining steps. For IrO_2 the Tafel slope changed linearly with the temperature, which indicates that the determining step in OER did not change with the temperature. For Co_3O_4, the Tafel slope changes from the maximum value (111 mV dec^{-1}) at room temperature to the minimum value (61 mV dec^{-1}) at a moderate temperature, meaning that the change of rate-determining from step I (OH^- adsorption) to a mixed mode with both step I and step II (O−H bond breaking). In addition, the fastest kinetics at a moderate temperature was observed for different electrolyte (KOH) concentrations and other Co-based catalysts, which is valuable for the practical application of water-splitting. By harnessing the temperature effect, we designed a fully solar-powered water electrolyzer to utilize sunlight for both heating the electrolyte to a target temperature and providing electricity to split water from a solar cell, as illustrated in Figure 1a.

RESULTS AND DISCUSSION

We first compared the gas conversion efficiency of commercial IrO_2 (purchased from Alfa) and Co_3O_4 (detailed synthesis and structure shown in experimental section and Figure S1 in Supporting Information (SI)) catalysts in electrolysis. The temperature of the electrolyte was monitored by thermometer (Figure 1a). When the potential was set at 1.52 V vs RHE, there was little gas generated. Interestingly, after exposure to simulated sunlight for 0.5 h, the gas conversion efficiencies on two electrodes were obviously increased. The thermometer showed that the temperature of the electrolyte increased from room temperature to 65 °C because of the light radiation, especially from the infrared part of the spectrum. The temperature remained at around 65 °C, and the bubbling rate remained constant. This experiment showed that the temperature plays a significant role in water electrolysis. Next, we systematically studied the temperature effect on the OER performance with IrO_2 and Co_3O_4 catalysts in the water-splitting process.

We then compared the OER performance of both catalysts at room temperature of 25 and 65 °C by linear sweep voltammetry. The potentials were converted to that with reference to the reversible hydrogen electrode (E_{RHE}, calculation method is shown in the experimental section and Figures S2 and S3 in SI) with temperature compensation. Figure 1b presents that the potentials of both catalysts at 10 mA cm^{-2} were ∼1.54 V vs RHE at 25 °C; as the temperature increased to 65 °C, their potentials decreased to ∼1.45 V vs RHE, and at 1.54 V vs RHE the current density of Co_3O_4 reached 200 mA cm^{-2}. Meanwhile, it can be observed that at 25 °C the current density of IrO_2 at 1.64 V vs RHE is higher than that of Co_3O_4. In contrast, at 65 °C the current density of

DOI: 10.1021/acs.inorgchem.7b03168
Inorg. Chem. 2018, 57, 2766−2772

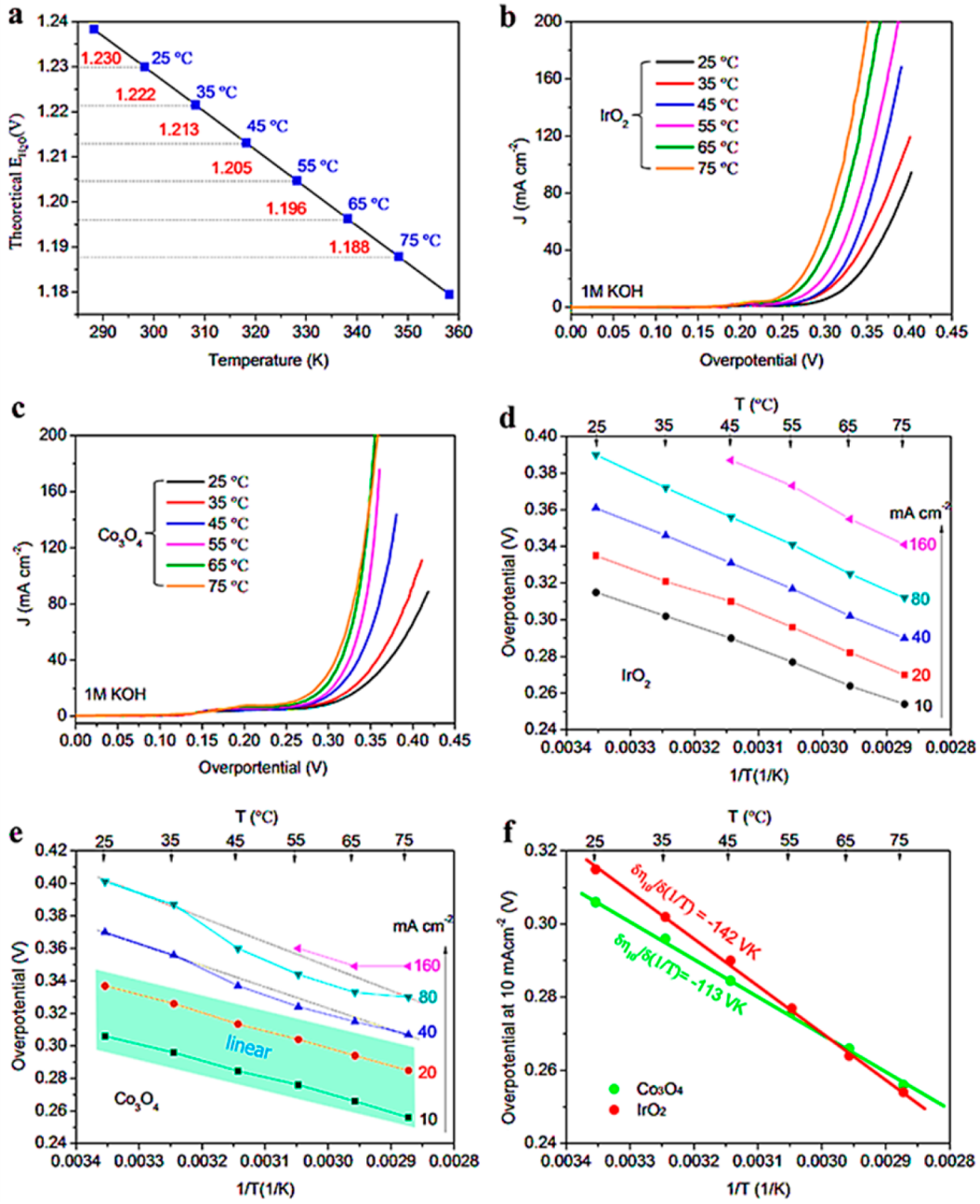

Figure 2. (a) Theoretical decomposition potential of H_2O plotted against temperature (T). (b, c) LSV curves with overpotentials (η) and (d, e) overpotentials (η) plotted against the reciprocal of temperature ($1/T$) of (b, d) IrO_2 and (c, e) Co_3O_4 catalysts at different current densities of 10, 20, 40, 80, and 160 mA cm^{-2}, (f) the compared overpotentials (η) of both catalysts at current density of 10 mA cm^{-2}.

Co_3O_4 at 1.55 V vs RHE is higher than that of IrO_2, showing the better OER performance of Co_3O_4 at a high temperature. In addition, the catalytic kinetics was further analyzed. Figure 1c shows the Tafel plots of Co_3O_4 and IrO_2 catalysts at different temperatures. With the increase of the temperature from 25 to 65 °C, the Tafel slope of IrO_2 deceases from 73 to 63 mV dec^{-1}, corresponding to 0.25 mV dec^{-1} per degree, while Co_3O_4 showed a Tafel slope of 111 mV dec^{-1} (Table S1 shows this value is consistent with that of the reported Co_3O_4 in recent years) at a room temperature of 25 °C, and at 65 °C its Tafel slope decreased rapidly to 61 mV dec^{-1}. The descendent rate of 1.27 mV dec^{-1} per degree is ~5 times higher than that of IrO_2. These results demonstrate that on Co_3O_4 the activity has a more sensitive dependence on the temperature.

In order to figure out the role of the temperature in OER with catalysts, the relationship between η and temperature needs to be explored. First, the calculation of η needs to be based on the theoretical decomposition potential of H_2O (E_{H_2O}), which depends linearly on the temperature, as shown in Figure 2a (the calculation method is shown in experimental section in SI). It can be seen that the E_{H_2O} value decreases as the temperature rises. The η value is the difference between the E_{RHE} (the calibration LSV curves with E_{RHE} are shown in Figure S5) and E_{H_2O} value at a specific temperature. Figure 2b,c shows the LSV curves with calculated η values of IrO_2 and Co_3O_4

DOI: 10.1021/acs.inorgchem.7b03168
Inorg. Chem. 2018, 57, 2766−2772

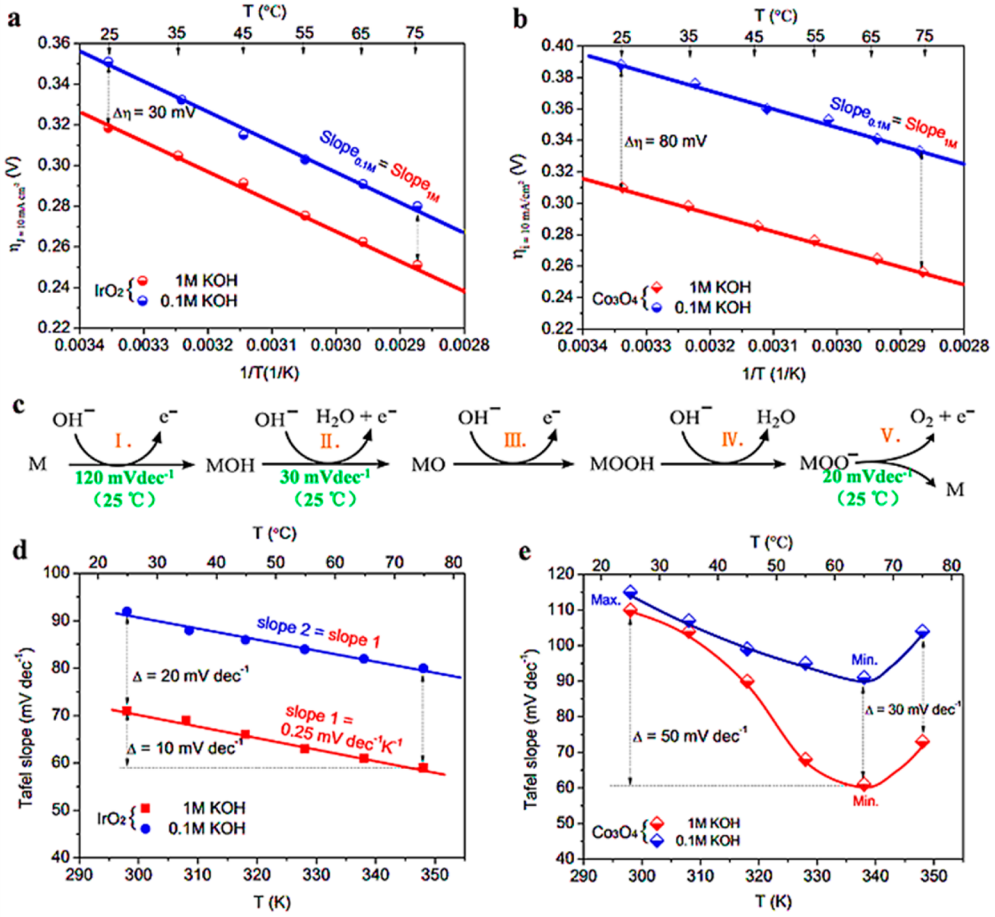

Figure 3. (a, b) Overpotentials at 10 mA cm^{-2} (η_{10}) plotted against the reciprocal of temperature ($1/T$) of (a) IrO_2 and (b) Co_3O_4 in 1 and 0.1 M KOH, (c) proposed OER pathway on the surface of catalyst with intermediates MOH, MO, MOOH, and MOO^-, (d, e) Tafel slope values plotted against temperature (T) of (d) IrO_2 and (e) Co_3O_4 catalysts in 1 and 0.1 M KOH.

catalysts at different temperatures from 25 to 75 °C with an error of ±1 °C. It can be observed that in both catalytic systems the onset η gradually decreases with the temperature increasing.

Especially, for Co_3O_4 catalyst, the η_{200} at a high current density of 200 mA cm^{-2} showed an abnormal temperature dependence that the η_{200} value at 65 °C is more negative than that at 75 °C. Furthermore, by plotting η against $1/T$ at different current densities of 10, 20, 40, 80, and 160 mA cm^{-2}, it can be observed from Figure 2d that there is a linear relationship between η and $1/T$ at all current densities for IrO_2. However, for Co_3O_4, the linear relationship only holds at low current densities of ≤20 mA cm^{-2} (Figure 2e). It can be observed from Figure 2f that the slope of the Co_3O_4 catalyzed system is −113 VK, higher than that (−142 VK) of the IrO_2 system, which presents the different catalytic activities of IrO_2 and Co_3O_4 catalysts. At current densities of 40 and 80 mA cm^{-2}, the η values of Co_3O_4 at moderate temperatures of 45, 55, and 65 °C are below the trendline (dashed line in Figure 2e). More strikingly, at a higher 160 mA cm^{-2}, the η at 75 °C is equal to that at 65 °C. Therefore, we concluded that the temperature effect is different in the IrO_2 and Co_3O_4 catalytic OER systems.

Next, we further investigated the difference in the temperature effect for both catalytic systems by changing the electrolyte concentration. Decades of research[20−23] have shown that in an alkaline electrolyte, hydroxide anions first adsorb on the surface of the catalyst and become the main reactant species, the concentration of which restricts the η (activity) and the Tafel slope (kinetics) during OER process. We tested the OER performance of both IrO_2 and Co_3O_4 catalysts in a 0.1 M KOH solution (their LSV curves are shown in Figure S6). Figure 3a,b compares η_{10} plotted against $1/T$ at 10 mA cm^{-2} for IrO_2 and Co_3O_4 in 1 and 0.1 M KOH. It can be observed that the slopes of both catalysts in 0.1 M KOH are the same as those in 1 M KOH, demonstrating that the constant slope value is only related to the catalyst and represents the intrinsic catalytic activity. Furthermore, for both catalysts, the differences of η_{10} at the different temperatures between 0.1 and 1 M KOH are constants, but the $\Delta\eta_{10}$ ($= \eta_{0.1M} - \eta_{1M}$) value (80 mV) of Co_3O_4 is much higher than that (30 mV) of IrO_2, demonstrating that the catalytic activity of Co_3O_4 is more dependent on the concentration of the hydroxides.

Figure 3c shows the proposed OER mechanism under an alkaline condition. The mechanism is based on the literature,[24,25] and it considerS OER with hydroxide anions. For multistep reaction mechanism, the Tafel slope (b) is defined as the dependency of the *iR*-corrected η (EIS in Figures S7 and S8) on the current density (J) as follows:[26,27]

$$\frac{1}{b} = \frac{\partial \lg(J)}{\partial \eta} = \frac{2.303RT}{azF} \quad (1)$$

where R is the ideal gas constant (8.314 J K^{-1} mol^{-1}), F is the Faraday constant (96485 J V^{-1} mol^{-1}), α and z are the transfer

DOI: 10.1021/acs.inorgchem.7b03168
Inorg. Chem. 2018, 57, 2766−2772

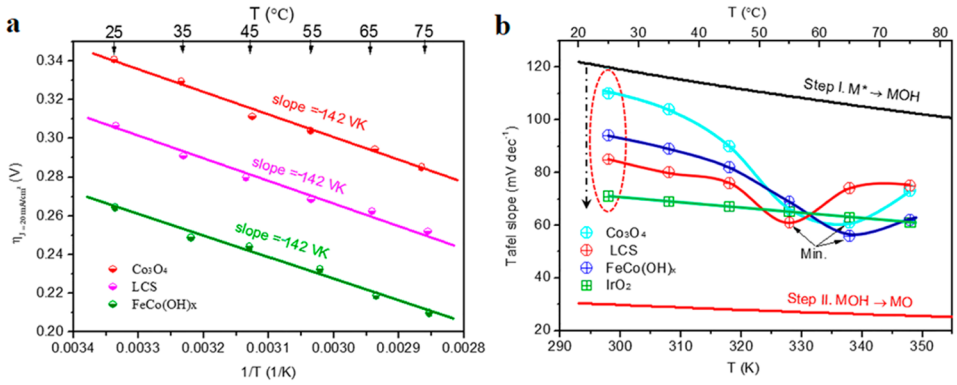

Figure 4. (a) Overpotentials (η_{20}) at 20 mA cm^{-2} plotted against reciprocal of temperature ($1/T$) and (b) Tafel slopes plotted against temperature (T) for three Co-based catalysts (Co_3O_4, Li_2CoSiO_4, and Fe-doped $Co(OH)_x$) in 1 M KOH.

coefficient and the number of transferred electrons in the rate-determining step, respectively. It is well-known that the OER reaction rate is determined by a multiple reaction step. The main rate-determining steps include OH^- adsorption (step I), O−H bond breaking (step II), and O_2 desorption (step V), which correspond to the theoretical Tafel slope values of 120 mV dec^{-1}, 30 mV dec^{-1}, and 20 mV dec^{-1} at room temperature of 25 °C, respectively.[23] Figure 3d,e shows the Tafel slope values (Tafel plots shown in Figures S5 and S6) plotted against the temperature for IrO_2 and Co_3O_4 catalysts in 1 and 0.1 M KOH. It can be observed that all the Tafel slope values at 25 °C are between 120 and 30 mV dec^{-1}, indicating the rate-determining step is mixed by OH^- adsorption (step I) and O−H bond breaking (step II). And interestingly, the Tafel slopes of IrO_2 and Co_3O_4 exhibit different dependence on the temperature. For THE IrO_2 system, Tafel slopes in 0.1 and 1 M KOH have a parallel linear relationship with the temperatures with a small change of $\Delta \approx 10$ mV dec^{-1}, indicating the rate-determining step does not change with the temperature. In addition, the Tafel slope (71−60 mV dec^{-1}) in 1 M KOH is 20 mV dec^{-1} lower than that (91−80 mV dec^{-1}) in 0.1 M KOH, demonstrating that OER kinetics is accelerated with the increase of OH^- concentration. However, for the Co_3O_4 system, there is a nonlinear variation with the temperature with a large change ($\Delta \approx 50$ mV dec^{-1}) in 1 M KOH, suggesting the change of the rate-determining step. The change of the rate-determining step can be attributed to that the changes in the rates of step I and step II with regard to the temperature are different in Co_3O_4 system. At room temperature of 25 °C, the Tafel slope value of 111 mV dec^{-1} demonstrates that OH^- adsorption (step I) is the main rate-determining step. The Tafel slope value of 61 mV dec^{-1} at a moderate temperature of 65 °C suggests that the rate-determining step shifts toward the O−H bond breaking (step II). At a temperature higher than 65 °C the main rate-determining step goes back to that of step I. Figure 3d,e further shows that for both catalysts the dependences of the Tafel slope on the temperature are similar at different electrolyte (KOH) concentrations.

To figure out structure stability of Co_3O_4 with temperature variation, the in situ XRD heating experiments of the Co_3O_4 were first carried out. As shown in Figure S9a, the phase structure of Co_3O_4 does not change with the temperature rise, which illustrates the stable structure of Co_3O_4 from 25 to 75 °C with almost unchanged lattice parameters vs temperatures (Figure S9b). However, it has been reported that during OER at high potential and at high pH, the surface of Co_3O_4 is corroded to form cobalt oxyhydroxide (CoOOH) active sites.[33] We also investigated the corrosion of Co_3O_4 after OER by phase structure and surface analysis. It can be seen in Figure S10 that the major phases of the samples after OER still correspond to the pristine Co_3O_4. XPS surface analysis in Figure S11 shows that the ratio of Co^{2+}/Co^{3+} in Co_3O_4 sample before OER is 1.23, while the ratios of Co^{2+}/Co^{3+} in Co_3O_4 samples after OER at 25 and 65 °C are 0.43 and 0.42, respectively, which are nearly the same to support that the corrosion of Co_3O_4 at higher temperature of 65 °C is almost the same as that at room temperature of 25 °C. In addition, Figure S8c shows that the OER performance of Co_3O_4 at 25-back °C (25-back °C: temperature changes from 75 °C back to 25 °C) is closed to that at initial 25 °C, which also verifies the structure stability of CoOOH active sites on the surface of Co_3O_4 after OER at high temperature.

We further confirmed that the dependence of η and Tafel slope on the temperature can be observed in other Co-based catalysts. Besides Co_3O_4, other two kinds of Co-based catalysts, Li_2CoSiO_4 (denoted as LCS, detailed synthesis, structure, and OER performance are shown in experimental section, Figure S12 and S14 in SI) and $FeCo(OH)_x$ (detailed synthesis, structure, and OER performance are shown in experimental section, Figures S13 and S14 in SI) were synthesized and used to catalyze water oxidation in 1 M KOH. The relationship between η_{20} and $1/T$ at 20 mA cm^{-2} is approximately linear as shown in Figure 4a. The slopes for Co_3O_4, LCS, and $FeCo(OH)_x$ are all around −142 VK, which can be attributed to the same Co active sites in the Co-based catalysts. And the temperature effect can be used as an indicator to identify which element plays a catalytic role in a multimetal catalyst, such as Fe/Ni/Co/W/Mo doped hydroxides and oxides. In addition, the temperature effect on the Tafel slope of Co_3O_4, LCS, and $FeCo(OH)_x$ was also investigated and shown in Figure 4b. First, it can be observed that the Tafel slope values of all Co-based catalysts at room temperature of 25 °C are larger than that of IrO_2 and closer to the theoretical line of step I, showing that the OH^- adsorption on Co-based catalysts is the rate-determining step. Second, with the change of the temperature, the Tafel slope values of all Co-based catalysts show similar nonlinear variation, indicating a similar temperature effect on the OER kinetics. Third, all Co-based catalysts show similar Tafel slopes (~60 mV dec^{-1}) in a moderate temperature range (55−65 °C), demonstrating that these Co-based catalysts have the same determining step in that temperature range.

DOI: 10.1021/acs.inorgchem.7b03168
Inorg. Chem. 2018, 57, 2766−2772

In summary, we report that in IrO_2 and Co_3O_4 catalytic systems the dependences of OER onset η on $1/T$ were different, and the slope at a low current density of 20 mA cm^{-2} was proven to be closely associated with their active sites. We had further observed that comparing to room temperature of 25 °C the OER performance of Co_3O_4 catalyst overtook that of IrO_2 at 65 °C, which was attributed to the different mechanisms of temperature effect on IrO_2 and Co_3O_4 catalysts. The Tafel slopes of IrO_2 change linearly with the temperature, suggesting that the rate-determining step does not change with the temperature. Co_3O_4 showed a larger change in the Tafel slope from the maximum value (~111 mV dec^{-1}) at room temperature to the minimum value (~61 mV dec^{-1}) at a moderate temperature, meaning that the changes from step I (OH^- adsorption) to a mixed mode including step I and step II (O−H bond breaking) is possible rate-determining step. We further demonstrated the temperature effect on η and the Tafel slope of Co_3O_4 can be extended to different electrolyte (KOH) concentrations and other Co-based catalysts. Our work establishes a link between the temperature and OER performance and contributes to optimize the performance of Co-catalysts in practical applications.

■ ASSOCIATED CONTENT

Supporting Information

The Supporting Information is available free of charge on the ACS Publications website at DOI: 10.1021/acs.inorgchem.7b03168.

Details of the experimental section, structure characterization of three Co-based catalysts (Co_3O_4, Li_2CoSiO_4, and Fe-doped $Co(OH)_x$), LSV curves, and Tafel plots at different temperatures and calculated methods of E_{RHE}, E_{H_2O}, and overpotentials (PDF)

■ AUTHOR INFORMATION

Corresponding Author

*E-mail: panfeng@pkusz.edu.cn.

ORCID

Feng Pan: 0000-0002-8216-1339

Author Contributions

†G.Z. and H.W. contributed equally.

Funding

The research was financially supported by National Science Foundation of China (No. 51602009), Postdoctoral Science Foundation of China (2016M600008), Natural Science Foundation of Guangdong Province (2015A030310138) and Shenzhen and Guangdong Research Grant (No. JCYJ20160226105838578 and 2015B090927003) .

Notes

The authors declare no competing financial interest.

■ ACKNOWLEDGMENTS

The research was financially supported by National Science Foundation of China (No. 51602009), Postdoctoral Science Foundation of China (2016M600008), National Materials Genome Project of China (2016YFB0700600) and Natural Science Foundation of Guangdong Province (2015A030310138).

■ REFERENCES

(1) Dresselhaus, M. S.; Thomas, I. L. Alternative Energy Technologies. *Nature* **2001**, *414*, 332−337.

(2) Gray, H. B. Powering the Planet with Solar Fuel. *Nat. Chem.* **2009**, *1*, 7−7.

(3) Liang, Y.; Li, Y.; Wang, H.; Zhou, J.; Wang, J.; Regier, T.; Dai, H. Co_3O_4 Nanocrystals on Graphene as a Synergistic Catalyst for Oxygen Reduction Reaction. *Nat. Mater.* **2011**, *10*, 780−786.

(4) Jiao, F.; Frei, H. Nanostructured Cobalt and Manganese Oxide Clusters as Efficient Water Oxidation Catalysts. *Energy Environ. Sci.* **2010**, *3*, 1018−1027.

(5) Gao, M. R.; Xu, Y. F.; Jiang, J.; Zheng, Y. R.; Yu, S. H. Water Oxidation Electrocatalyzed by an Efficient $Mn_3O_4/CoSe_2$ Nanocomposite. *J. Am. Chem. Soc.* **2012**, *134*, 2930−2933.

(6) Li, D.; Baydoun, H.; Verani, C. N.; Brock, S. L. Efficient Water Oxidation Using CoMnP Nanoparticles. *J. Am. Chem. Soc.* **2016**, *138*, 4006−4009.

(7) Lee, Y.; Suntivich, J.; May, K. J.; Perry, E. E.; Shao-Horn, Y. Synthesis and Activities of Rutile IrO_2 and RuO_2 Nanoparticles for Oxygen Evolution in Acid and Alkaline Solutions. *J. Phys. Chem. Lett.* **2012**, *3*, 399−404.

(8) Lu, X.; Zhao, C. Electrodeposition of Hierarchically Structured Three-Dimensional Nickel−Iron Electrodes for Efficient Oxygen Evolution at High Current Densities. *Nat. Commun.* **2015**, *6*, No. 6616, DOI: 10.1038/ncomms7616.

(9) Gong, M.; Dai, H. A Mini Review of NiFe-Based Materials as Highly Active Oxygen Evolution Reaction Electrocatalysts. *Nano Res.* **2015**, *8*, 23−39.

(10) Jiao, F.; Frei, H. Nanostructured Cobalt Oxide Clusters in Mesoporous Silica as Efficient Oxygen-Evolving Catalysts. *Angew. Chem., Int. Ed.* **2009**, *48*, 1841−1844.

(11) Xiao, X.; He, C. T.; Zhao, S.; Li, J.; Lin, W.; Yuan, Z.; Zhang, Q.; Wang, S.; Dai, L.; Yu, D. A General Approach to Cobalt-Based Homobimetallic Phosphide Ultrathin Nanosheets for Highly Efficient Oxygen Evolution in Alkaline Media. *Energy Environ. Sci.* **2017**, *10*, 893−899.

(12) Fominykh, K.; Chernev, P.; Zaharieva, I.; Sicklinger, J.; Stefanic, G.; Döblinger, M.; Müller, A.; Pokharel, A.; Böcklein, S.; Scheu, C.; Bein, T.; Fattakhova-Rohlfing, D. Iron-Doped Nickel Oxide Nanocrystals as Highly Efficient Electrocatalysts for Alkaline Water Splitting. *ACS Nano* **2015**, *9*, 5180−5188.

(13) Zhang, B.; Zheng, X.; Voznyy, O.; Comin, R.; Bajdich, M.; García-Melchor, M.; Han, L.; Xu, J.; Liu, M.; Zheng, L.; García de Arquer, F. P.; Dinh, C. T.; Fan, F.; Yuan, M.; Yassitepe, E.; Chen, N.; Regier, T.; Liu, P.; Li, Y.; De Luna, P.; Janmohamed, A.; Xin, H. L.; Yang, H.; Vojvodic, A.; Sargent, E. H. Homogeneously Dispersed Multimetal Oxygen-Evolving Catalysts. *Science* **2016**, *352*, 333−337.

(14) Zhang, G.; Yang, J.; Wang, H.; Chen, H.; Yang, J.; Pan, F. $Co_3O_{4-\delta}$ Quantum Dots as a Highly Efficient Oxygen Evolution Reaction Catalyst for Water Splitting. *ACS Appl. Mater. Interfaces* **2017**, *9*, 16159−6167.

(15) Ma, T. Y.; Dai, S.; Jaroniec, M.; Qiao, S. Z. Metal-Organic Framework Derived Hybrid Co3O4-Carbon Porous Nanowire Arrays as Reversible Oxygen Evolution Electrodes. *J. Am. Chem. Soc.* **2014**, *136*, 13925−13931.

(16) Kuo, D. Y.; Kawasaki, J. K.; Nelson, J. N.; Kloppenburg, J.; Hautier, G.; Shen, K. M.; Schlom, D. G.; Suntivich, J. Influence of Surface Adsorption on the Oxygen Evolution Reaction on IrO_2 (110). *J. Am. Chem. Soc.* **2017**, *139*, 3473−3479.

(17) Görlin, M.; Ferreira de Araújo, J.; Schmies, H.; Bernsmeier, D.; Dresp, P.; Gliech, M.; Jusys, Z.; Chernev, P.; Kraehnert, R.; Dau, h.; Strasser, P. Tracking Catalyst Redox States and Reaction Dynamics in Ni-Fe Oxyhydroxide Oxygen Evolution Reaction Electrocatalysts: The Role of Catalyst Support and Electrolyte pH. *J. Am. Chem. Soc.* **2017**, *139*, 2070−2082.

(18) Shinagawa, T.; Ng, M. T.-K.; Takanabe, K. Boosting the Performance of the Nickel Anode in the Oxygen Evolution Reaction by Simple Electrochemical Activation. *Angew. Chem., Int. Ed.* **2017**, *56*, 5061−5065.

DOI: 10.1021/acs.inorgchem.7b03168
Inorg. Chem. 2018, 57, 2766−2772

(19) Koehl, M.; Heck, M.; Wiesmeier, S.; Wirth, J. Modeling of the Nominal Operating Cell Temperature Based on Outdoor Weathering. *Sol. Energy Mater. Sol. Cells* **2011**, *95*, 1638−1646.
(20) Trotochaud, L.; Ranney, J. K.; Williams, K. N.; Boettcher, S. W. Solution-Cast Metal Oxide Thin Film Electrocatalysts for Oxygen Evolution. *J. Am. Chem. Soc.* **2012**, *134*, 17253−17261.
(21) Yu, X.; Zhang, M.; Yuan, W.; Shi, G. High-Performance Three-Dimensional Ni-Fe Layered Double Hydroxide/Graphene Electrode for Water Oxidation. *J. Mater. Chem. A* **2015**, *3*, 6921−6928.
(22) Louie, M. W.; Bell, A. T. An Investigation of Thin-Film Ni-Fe Oxide Catalysts for the Electrochemical Evolution of Oxygen. *J. Am. Chem. Soc.* **2013**, *135*, 12329−12337.
(23) Shinagawa, T.; Garcia-Esparza, A. T.; Takanabe, K. Insight on Tafel slopes from a Microkinetic Analysis of Aqueous Electrocatalysis for Energy Conversion. *Sci. Rep.* **2015**, *5*, 13801−13822.
(24) Cui, X.; Ren, P.; Deng, D.; Deng, J.; Bao, X. Single Layer Graphene Encapsulating Non-Precious Metals as High-Performance Electrocatalysts for Water Oxidation. *Energy Environ. Sci.* **2016**, *9*, 123−129.
(25) Gao, M.; Sheng, W.; Zhuang, Z.; Fang, Q.; Gu, S.; Jiang, J.; Yan, Y. Efficient Water Oxidation Using Nanostructured α-Nickel-Hydroxide as an Electrocatalyst. *J. Am. Chem. Soc.* **2014**, *136*, 7077−7084.
(26) Fabbri, E.; Habereder, A.; Waltar, K.; Kotz, R.; Schmidt, T. J. Developments and Perspectives of Oxide-Based Catalysts for the Oxygen Evolution Reaction. *Catal. Sci. Technol.* **2014**, *4*, 3800−3821.
(27) Irshad, A.; Munichandraiah, N. An Oxygen Evolution Co-Ac Catalyst–The Synergistic Effect of Phosphate Ions. *Phys. Chem. Chem. Phys.* **2014**, *16*, 5412−5422.
(28) Zhou, P.; Wang, Y.; Xie, C.; Chen, C.; Liu, H.; Chen, R.; Huo, H.; Wang, S. Acid-Etched Layered Double Hydroxides with Rich Defects for Enhancing the Oxygen Evolution Reaction. *Chem. Commun.* **2017**, *53*, 11778−11781.
(29) Liu, R.; Wang, Y.; Liu, D.; Zou, Y.; Wang, S. Water-Plasma-Enabled Exfoliation of Ultrathin Layered Double Hydroxide Nanosheets with Multivacancies for Water Oxidation. *Adv. Mater.* **2017**, *29*, 1701546.
(30) Wang, Y.; Xie, C.; Zhang, Z.; Liu, D.; Chen, R.; Wang, S. In Situ Exfoliated, N-Doped, and Edge-Rich Ultrathin Layered Double Hydroxides Nanosheets for Oxygen Evolution Reaction. *Adv. Funct. Mater.* **2018**, *28*, 1703363.
(31) Xiao, Z.; Wang, Y.; Huang, Y.; Wei, Z.; Dong, C.; Ma, J.; Shen, S.; Li, Y.; Wang, S. Filling the Oxygen Vacancies in Co_3O_4 with Phosphorus: an Ultra-efficient Electrocatalyst for the Overall Water Splitting. *Energy Environ. Sci.* **2017**, *10*, 2563−2569.
(32) Dou, S.; Dong, C.; Hu, Z.; Huang, Y.; Chen, J.; Tao, L.; Yan, D.; Chen, D.; Shen, S.; Chou, S.; Wang, S. Atomic-Scale CoO_x Species in Metal-Organic Frameworks for Oxygen Evolution Reaction. *Adv. Funct. Mater.* **2017**, *27*, 1702546.
(33) Xu, L.; Jiang, Q.; Xiao, Z.; Li, X.; Huo, J.; Wang, S.; Dai, L. Plasma-engraved Co_3O_4 nanosheets with oxygen vacancies and high surface area for the oxygen evolution reaction. *Angew. Chem., Int. Ed.* **2016**, *55*, 5277.

DOI: 10.1021/acs.inorgchem.7b03168
Inorg. Chem. 2018, 57, 2766−2772